

## Acoustoconductivity of quantum wires

M. Blencowe

*The Blackett Laboratory, Imperial College of Science, Technology and Medicine, London SW7 2BZ, United Kingdom*

A. Shik

*A. F. Ioffe Physical-Technical Institute, 194021 St. Petersburg, Russia*

(Received 23 April 1996)

The change in conductivity of quantum wires under the influence of nonequilibrium phonons is considered theoretically. The particular mechanism of this acoustoconductivity (AC) depends on the wire length  $L$ . For long wires with  $L$  exceeding the localization length, the main effect involves the phonon-induced partial delocalization of carriers. In this case AC will be positive. The electron-phonon scattering rate and, hence, the amplitude of AC, oscillates with the electron density in a wire, having maxima when the Fermi level coincides with the edge of some one-dimensional subband. All these regularities are in agreement with the recent experimental data. In the case of short, ballistic wires, nonequilibrium phonons cause additional backscattering of carriers and AC must be negative. [S0163-1829(96)00943-5]

### I. INTRODUCTION

Nonequilibrium ballistic phonon pulses have been successfully used to probe the properties of low-dimensional electron systems, providing information on, for example, the electron spectrum and scattering processes (see, e.g., Ref. 1). Among the various phonon pulse techniques, an important place belongs to acoustoconductivity (AC), the change in the conductivity under the influence of nonequilibrium phonons. Scanning AC, or ‘‘phonon imaging,’’<sup>2</sup> has been used so far to investigate the electron-phonon interaction in a two-dimensional electron gas, particularly under the quantum Hall effect conditions.<sup>3</sup>

Recently, the first results of AC measurements in structures with a quasi-one-dimensional electron gas (quantum wires) have appeared.<sup>4</sup> They demonstrated that for quasiballistic wires where the equilibrium conductivity  $\sigma_0$  vs Fermi energy  $E_F$  dependence exhibited steps which were not very well pronounced, AC had a positive sign and strong oscillations as a function of  $E_F$ . In the present paper, we present a physical picture of AC which provides, in particular, a possible explanation of the experimental results of Ref. 4 and predicts some new regularities.

### II. ELECTRON-PHONON INTERACTION

In order to describe the properties of AC, we must first of all consider the electron-acoustic phonon interaction in quantum wires. The analogous problem for equilibrium phonons has already been considered by several authors.<sup>5-9</sup> In the papers devoted to the energy relaxation problem,<sup>10,11</sup> where processes of phonon emission dominate over those of absorption, similar calculations have been made for a nonequilibrium distribution of hot electrons. In our case, the situation is in some sense the opposite: we have an equilibrium electron distribution at a low temperature and a nonequilibrium phonon system so that the phonon emission can be neglected compared to the absorption.

We consider a quantum wire formed by some lateral con-

fining potential  $U(x)$  in a two-dimensional electron system occupying the plane  $z=0$ . The energy spectrum and wave functions of the wire are

$$E = E_N + \frac{\hbar^2 k^2}{2m}, \quad (1)$$

$$\Psi = \exp(iky) \psi_0(z) u_N(x), \quad (2)$$

where  $k$  is the wave vector along the wire ( $y$  axis),  $E_N$  ( $N=0,1,2,\dots$ ) are the energy levels in the confining potential  $U(x)$  corresponding to the wave functions  $u_N(x)$ , and  $\psi_0(z)$  is the ground state wave function for the two-dimensional electron gas formed by strong confinement in the  $z$  direction.

For electrons with isotropic effective mass the interaction with acoustic phonons with wave vector  $\mathbf{q}$  is described by the potential  $V_{\mathbf{q}} = (Cq^\gamma/\Omega)^{1/2} \exp(i\mathbf{q} \cdot \mathbf{r})$ , where  $\Omega$  is the normalizing volume,  $\gamma=+1$  for deformation coupling and  $-1$  for piezoelectric coupling. Interaction constants  $C$  for both types of interaction may be found, for example, in Ref. 12. The corresponding matrix elements can be easily calculated:

$$\langle N, k | V_{\mathbf{q}} | M, k' \rangle = (Cq^\gamma/\Omega)^{1/2} \delta_{k'; k+q_y} Z(q_z) Q_{MN}(q_x). \quad (3)$$

Here  $Z(q_z) = \int dz \psi_0^2(z) \exp(iq_z z)$  and  $Q_{MN}(q_x) = \int dx u_M^*(x) u_N(x) \exp(iq_x x)$  are the form-factors suppressing the electron-phonon interaction for large  $q_x$  and  $q_z$  exceeding the inverse wire width  $a$  and thickness  $b$  in  $x$  and  $z$  directions, respectively. We are considering the typical situation for quantum wires where  $a > b$  and the lateral quantization in  $x$  direction is weaker than that in the  $z$  direction.

As a characteristic of electron-phonon scattering in the wire, we consider the scattering probability  $W_N(k)$  for an electron with quantum numbers  $N$  and  $k$  given by

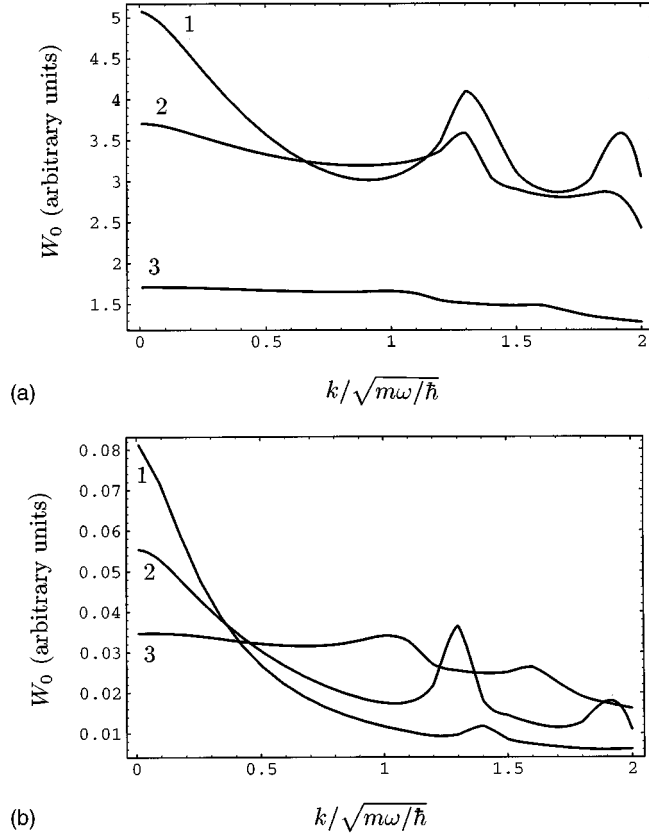


FIG. 1. Phonon scattering probability  $W_0(k)$  (arbitrary units) for the ground subband of a quantum wire with parabolic confining potential  $U(x) = m\omega^2 x^2/2$  and deformation coupling ( $\gamma = +1$ ). The dimensionless temperature  $T_h/m s^2$  is equal to  $10^2$  (a) and 10 (b). The wave vector  $k$  is given in units of  $\sqrt{m\omega/\hbar} = a^{-1}$ , so that the electron energy coincides with the  $M$ th subband edge when  $k = \sqrt{2M}$ . The wire width parameter  $s\sqrt{m/\hbar\omega} = msa/\hbar$  is equal to 0.05 (curve 1), 0.1 (curve 2), and 0.3 (curve 3).

$$W_N(k) = \frac{C}{(2\pi)^2 \hbar} \times \sum_M \int \int \int \mathbf{d}^3 \mathbf{q} \, q^\gamma F(\mathbf{q}) |Z(q_z)|^2 |Q_{MN}(q_x)|^2 \delta \left( E_N - E_M - \frac{\hbar^2 k q_y}{m} - \frac{\hbar^2 q_y^2}{2m} + \hbar s q \right), \quad (4)$$

where  $s$  is the sound velocity. As has already been mentioned, we neglect phonon emission processes.

To obtain the explicit formula for  $W_N(k)$ , we must specify the phonon distribution function  $F(\mathbf{q})$ . We consider two different models for  $F(\mathbf{q})$ .

### A. Isotropic Bose distribution

As our first model, we assume  $F(\mathbf{q})$  to be an isotropic Bose function with some effective heater temperature  $T_h$ :  $F(\mathbf{q}) = N(q) \equiv [\exp(\hbar s q/T_h) - 1]^{-1}$ . For  $T_h < \hbar s/a$ , where  $a$  is the wire width, the dominant wavelength phonons cannot cause interlevel transitions and we may make the approximation  $Q_{MN} = \delta_{MN}$ . Since  $b < a$ , for such phonons  $q_z b < 1$  so that  $Z(q_z) = 1$ . The expression for  $W_N(k)$  then becomes very simple:

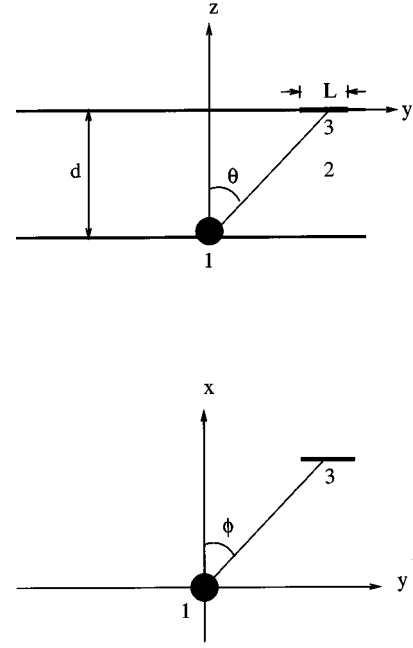


FIG. 2. Schematic picture of experiments on AC in quantum wires. 1—hot spot; 2—substrate; 3—quantum wire.

$$W_N(k) = \frac{Cm}{2\pi\hbar^3} \left[ \int_{\max\{0; 2ms/\hbar - 2k\}}^{2k + 2ms/\hbar} \frac{dq \, q^{\gamma+1} F(q)}{\sqrt{k^2 + 2msq/\hbar}} + 2 \int_{2k + 2ms/\hbar}^{\infty} \frac{dq \, q^{\gamma+1} F(q)}{\sqrt{k^2 + 2msq/\hbar}} \right]. \quad (5)$$

This expression acquires its maximum value at  $k \rightarrow 0$  (near the subband edge) and decreases monotonically with increasing  $k$ .

At higher  $T_h$  the  $W_N$  vs  $k$  dependence becomes nonmonotonic, having maxima near  $k = [\sqrt{2m(E_M - E_N) + m^2 s^2} - ms]/\hbar$ , where an additional scattering channel into the  $M$ th subband becomes available. The  $W_N$  vs  $k$  dependence at different  $T_h$  and  $a$  is given in Fig. 1 for the case of deformation coupling ( $\gamma = 1$ ). For piezoelectric coupling ( $\gamma = -1$ ), Eq. (4) with isotropic Bose function diverges at  $q \rightarrow 0$ , so that the Debye screening and/or disorder broadening must additionally be taken into account. We are more interested in deformation coupling since it is connected with larger  $q$  and, hence, with larger energy transfer and is more effective in phase relaxation processes responsible for AC (see Sec. V).

### B. Narrow-angle Bose distribution

In experiments on phonon imaging,<sup>2</sup> nonequilibrium phonons are generated locally at some point on the opposite side of the substrate by a focused laser beam or a small resistive heater (Fig. 2). If the dimensions of this hot spot as well as of the quantum wire are much less than the substrate thickness  $d$ , we may assume that all phonons reaching the wire have almost the same momentum direction which can be varied by scanning the hot spot. This means that  $F(q, \theta, \phi) \sim \delta(\theta - \theta_0) \delta(\phi - \phi_0) N(q)$ , where  $N(q)$  is the Bose function (see Sec. II A) and the angles  $\theta_0, \phi_0$  are determined by the hot spot position (see Fig. 2).

For an electron with quantum numbers  $N, k$ , the various possible transitions can be found in Fig. 3, where  $\alpha = \arctan(\hbar s/\xi)$  and  $\xi \equiv |\sin\theta_0 \sin\phi_0| = |q_y|/q$ . One can see that there exist two particular phonons with the wave vectors

$$\tilde{q}_{MN}^f(k) \equiv \frac{1}{\xi} [(-k + ms/\hbar\xi) + \sqrt{(k - ms/\hbar\xi)^2 + 2m(E_N - E_M)/\hbar^2}] \quad (6)$$

and

$$\tilde{q}_{MN}^b(k) \equiv \frac{1}{\xi} [(k + ms/\hbar\xi) + \sqrt{(k + ms/\hbar\xi)^2 + 2m(E_N - E_M)/\hbar^2}], \quad (7)$$

causing, correspondingly, forward and backscattering into the  $M$ th subband ( $M \neq N$ ) [for intrasubband transitions ( $M = N$ ) forward scattering is possible only for  $\hbar k \xi < ms$ ]. Equation (4) gives

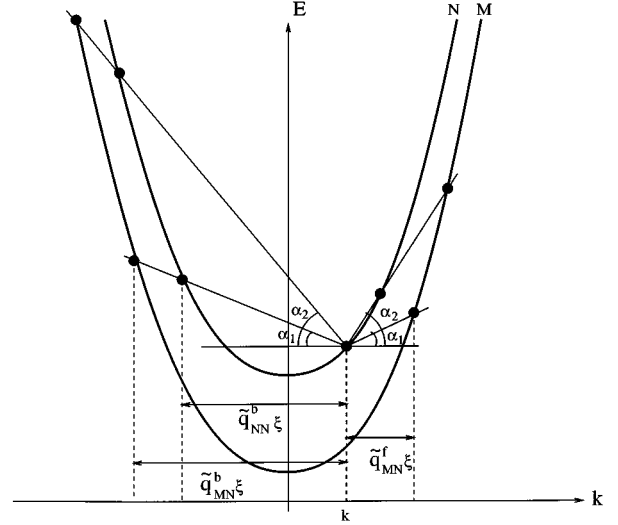


FIG. 3. Energy spectrum of a quantum wire and possible phonon-induced electron transitions. Intra- and intersubband transitions are shown for  $\hbar k \xi > ms$  ( $\alpha_1$ ) and  $\hbar k \xi < ms$  ( $\alpha_2$ ).

$$W_N(k) \sim \sum_M \frac{[\tilde{q}_{MN}^f(k)]^{\gamma+2} |Z(\tilde{q}_{MN}^f(k) \cos\theta_0)|^2 |Q_{MN}(\tilde{q}_{MN}^f(k) \sin\theta_0 \cos\phi_0)|^2}{\sqrt{(k - ms/\hbar\xi)^2 + 2m(E_N - E_M)/\hbar^2} [\exp(\hbar s \tilde{q}_{MN}^f(k)/T_h) - 1]} \quad (8)$$

for  $\phi > 0$  and

$$W_N(k) \sim \sum_M \frac{[\tilde{q}_{MN}^b(k)]^{\gamma+2} |Z(\tilde{q}_{MN}^b(k) \cos\theta_0)|^2 |Q_{MN}(\tilde{q}_{MN}^b(k) \sin\theta_0 \cos\phi_0)|^2}{\sqrt{(k + ms/\hbar\xi)^2 + 2m(E_N - E_M)/\hbar^2} [\exp(\hbar s \tilde{q}_{MN}^b(k)/T_h) - 1]} \quad (9)$$

for  $\phi < 0$ . Note that Eqs. (6)–(9) assume  $k > 0$ . To obtain the corresponding equations for  $k < 0$ , the superscripts  $b$  and  $f$  as well as conditions  $\phi > 0$  and  $\phi < 0$  should be interchanged. Figure 4 shows the resulting  $W_N$  vs  $k$  dependences for several different phonon incident angles (different  $\xi$ ).

### III. IDEAL BALLISTIC QUANTUM WIRES

Let us discuss briefly AC for an ideal quantum wire with only electron-phonon scattering. The assumption of ideality means that at low temperatures  $T$  the equilibrium conductance  $\sigma_0$  of a wire must have a ballistic character. It is well known (see, e.g., Ref. 13) that in this case

$$\sigma_0 = \frac{e^2}{\pi\hbar} \sum_N T_N \theta(E_F - E_N), \quad (10)$$

where  $E_N$  is the energy of the  $N$ th energy level and  $T_N$  is the transmission coefficient for electrons in the  $N$ th subband. At

zero temperature all  $T_N = 1$ . Their deviation from unity caused by equilibrium phonons at nonzero temperature was calculated in Refs. 14,15. To obtain the formula for AC  $\Delta\sigma$  in an ideal wire, we must derive the similar expression, but now for nonequilibrium phonon distributions.

For sufficiently small phonon density such that multiple electron-phonon scattering processes can be neglected, the electron transmission probability through the wire with length  $L$  is determined by the probability of a single backscattering event,  $W_N^b(k)$  (we are interested only in backscattering since in one-dimensional systems forward scattering does not influence the conductivity<sup>13</sup>), and is given by  $1 - LW_N^b(k)m/\hbar k$ . Here  $W_N^b(k)$  is determined by a formula similar to Eq. (4), where the integration over  $k_1$  is restricted to the interval  $(-\infty, 0)$ . Assuming electrons to be completely degenerate and calculating this expression at the Fermi energy, we obtain the coefficient  $T_N$  in Eq. (10) and, eventually,

$$\Delta\sigma = - \frac{e^2 L m C}{(2\pi)^3 \hbar^3} \sum_{MN} \frac{1}{\sqrt{E_F - E_N}} \int \int \frac{dq_x dq_z q^\gamma F(\mathbf{q}) |Z(q_z)|^2 |Q_{MN}(q_x)|^2}{\sqrt{E_F - E_M + \hbar s q}}. \quad (11)$$

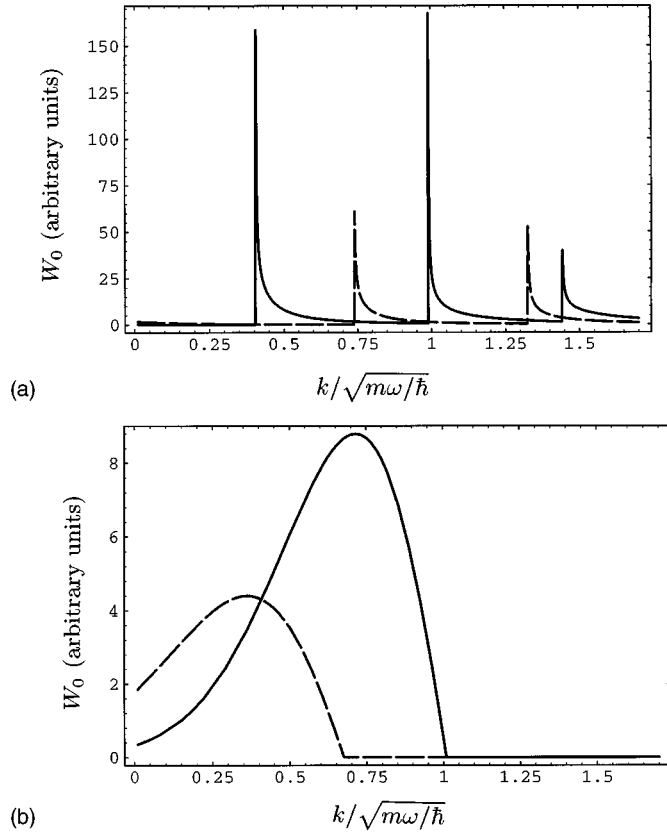


FIG. 4. Phonon scattering probability  $W_0(k)$  for the same wire as in Fig. 1 with  $T_h/ms^2=10^2$  and  $s\sqrt{m/\hbar}\omega=0.1$ , but for narrow-angle phonon distribution with  $\xi=0.1$  (solid curve) and  $\xi=0.15$  (dashed curve). (a)  $\phi < 0$ . (b)  $\phi > 0$ .

Here the  $y$  component of  $\mathbf{q}$  has a fixed value approximately (with neglect of the phonon energy) equal to  $-\sqrt{2m}(\sqrt{E_F-E_N}+\sqrt{E_F-E_M})/\hbar$ . This is virtually the same result which can be obtained from the expressions of Refs. 14,15 derived by the method of kinetic equation.

Not considering the expression in detail, we point out the two most important conclusions:

- (1) AC is always negative.
- (2) AC diverges at  $E_F \rightarrow E_N$ , that is at the subband edges.

The first result is evident since in the ideal case any scattering (in our case—by nonequilibrium phonons) can only decrease the coefficients  $T_N$ . But this contradicts the experimental data<sup>4</sup> where  $\Delta\sigma > 0$ . The second result is a consequence of the singularities in one-dimensional density of states and appears in calculations of the quantum wire conductivity which employ the simple Born approximation (see, e.g., Refs. 5, 16, and 17).

The divergencies occurring in the kinetic characteristics of an ideal model are an immanent property of a one-dimensional system and are connected with the fact that in the one-dimensional case, even weak elastic scattering causes localization of electron states and, hence, cannot be ignored in most cases. The important role of elastic scattering in the particular experiments<sup>4</sup> that we want to explain, is confirmed by the fact that the observed steps in the experimental  $\sigma_0$  vs  $E_F$  dependence were considerably smooth.

As a result, the adequate AC theory must inevitably take into account the elastic scattering of carriers by impurities and wire defects. This will be done in the next sections.

#### IV. EFFECTS OF ELASTIC SCATTERING

Prior to discussing the AC effect in a nonideal wire, we consider such a wire without phonon scattering and calculate the characteristic time of elastic scattering  $\tau_N(k)$  for an electron with wave vector  $k$  in the  $N$ th subband determining the width of a quantum level and the amplitude of peaks appearing in the density of states instead of singularities at the energies  $E=E_N$ . We shall describe these scatterers by their concentration  $N_i$  and the potential of a single scatterer  $V(\mathbf{r}) = \sum_{\mathbf{q}} V_{\mathbf{q}} \exp(i\mathbf{q} \cdot \mathbf{r})$ . In the Born approximation

$$\frac{1}{\tau_N(k)} = \frac{N_i \Omega^2}{(2\pi)^2 \hbar} \sum_M \int \mathbf{d}^3 \mathbf{q} |V_{\mathbf{q}}|^2 |Z(q_z)|^2 |Q_{MN}(q_x)|^2 \times \delta \left( E_N - E_M - \frac{\hbar^2 k q_y}{m} + \frac{\hbar^2 q_y^2}{2m} \right). \quad (12)$$

This expression gives  $\tau_N^{-1}(k) \rightarrow \infty$  as the Fermi energy approaches any subband edge and, hence, cannot be directly applied. There are some papers where this problem has been solved (mostly numerically) by taking into account multiple scattering.<sup>18-23</sup> We prefer to obtain maybe more crude but semianalytical results and for this reason will employ the so-called self-consistent Born approximation<sup>24</sup> (see, also Refs. 25,26).

The above-mentioned approximation is obtained by replacing the  $\delta$  function in (12) with a broadened density of states:

$$\frac{1}{\tau_N(k, E)} = \frac{N_i \Omega^2}{(2\pi)^2 \hbar} \sum_M \int \mathbf{d}^3 \mathbf{q} |V_{\mathbf{q}}|^2 |Z(q_z)|^2 |Q_{MN}(q_x)|^2 \times \Gamma_M(k - q_y, E), \quad (13)$$

where

$$\Gamma_M(k - q_y, E) := \pi^{-1} \frac{\hbar/2\tau_M(k - q_y, E)}{[E - E_M - \hbar^2(k - q_y)^2/2m]^2 + [\hbar/2\tau_M(k - q_y, E)]^2}. \quad (14)$$

Note,  $\tau_N$  is, in general, now a function of both  $k$  and  $E$ —treated as independent variables. The  $q_y$  integral is readily carried out if the  $q$  dependence of  $V$  is neglected (e.g., for a  $\delta$ -like impurity potential). In this case,  $\tau_N$  depends only on the total electron energy  $E$  and is to be found from the equation

$$\frac{1}{\tau_N(E)} \approx \frac{\sqrt{m}}{(2\pi\hbar)^2} N_{il} |V|^2 \sum_M \int \int dq_x dq_z |Z(q_z)|^2 |Q_{MN}(q_x)|^2 \frac{\left[ \sqrt{(E-E_M)^2 + \left(\frac{\hbar}{2\tau_M(E)}\right)^2} + E - E_M \right]^{1/2}}{\sqrt{(E-E_M)^2 + \left(\frac{\hbar}{2\tau_M(E)}\right)^2}}. \quad (15)$$

This self-consistent Born approximation is well defined for all  $E$  and expected to be reasonably accurate provided  $\hbar/\tau_N \ll E_{N+1} - E_N$  and the density of scatterers is sufficiently low such that multiple scattering processes can be neglected.

It is convenient to introduce the individual rate  $\tau_{NM}^{-1}(E)$  for an electron initially in the  $N$ th subband to scatter into the  $M$ th subband, so that (15) is written as

$$\frac{1}{\tau_N(E)} = \sum_M \frac{1}{\tau_{NM}(E)}. \quad (16)$$

From (15), we see that for a given energy  $E$ , the individual rates  $\tau_{NM}^{-1}(E)$  with  $E_M - E \gg \hbar/\tau_M$  can be neglected and thus the sum over  $M$  approximated by a finite sum. Furthermore,  $\tau_{NM}^{-1}(E)$  and hence  $\tau_N^{-1}(E)$  has a maximum at  $E = E_M$ , with the width of the peak depending on  $\hbar/\tau_M(E_M)$ . This is clearly demonstrated in Fig. 5, obtained by numerically solving Eq. (15).

In principle, for very high elastic scattering rates the formulas of Sec. II for  $W_N(k)$  become inadequate since we cannot calculate the electron-phonon matrix element using electron wave functions of an ideal wire. In this case, it would be more correct to use the more involved approach developed by Schmid<sup>27</sup> for the theory of the electron-phonon interaction in dirty metals. However, we may expect considerable deviations from the ideal wire formulas of Sec. II only in the case when the energy uncertainty  $\hbar/\tau_N$  exceeds typical phonon energies which are of the order  $\hbar k_{Fs}$  (where

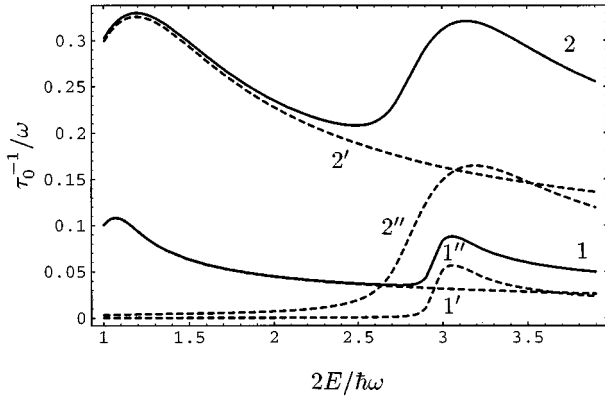


FIG. 5. Energy dependence of the elastic scattering probability  $\tau_0^{-1}(E)$ , obtained by self-consistent numerical calculations. The probability is given in units of  $\omega$  ( $=$  subband spacing/ $\hbar$ ), while  $E$  is given in units of  $\hbar\omega/2$ , so that subband edges are located at  $E = 2M + 1$ . The scattering strength  $N_{il}|V|^2$  is chosen such that  $\tau_0^{-1}(E_0) = 0.1\omega$  (curve 1) and  $\tau_0^{-1}(E_0) = 0.3\omega$  (curve 2). Also shown are the individual probabilities  $\tau_{00}^{-1}$  (curves 1', 2') and  $\tau_{01}^{-1}$  (curves 1'', 2'').

$k_F$  is the Fermi wave vector). We assume our wires to be of high enough quality so that this inequality does not take place.

## V. ACOUSTOCONDUCTIVITY IN A NONIDEAL QUANTUM WIRE

In the absence of inelastic processes the resistance of a wire depends on its length  $L$  according to Anderson's scaling expression:<sup>28</sup>

$$r(L) = r_s \left[ \exp\left(\frac{\rho_c L}{r_s}\right) - 1 \right] \equiv r_s [\exp(L/l_{loc}) - 1]. \quad (17)$$

Here  $r_s$  is the scaling resistance equal to  $2\pi\alpha\hbar/e^2$ , where  $\alpha$  is a numerical factor  $\approx 2$  and  $\rho_c$  is the classical resistivity per unit wire length equal to  $\pi\hbar(2e^2\Sigma_N l_N)^{-1}$  ( $l_N$  is the elastic mean free path in the  $N$ th subband). The formula is valid for nonballistic wires with  $L > l_N$ .

Inelastic, phase-breaking electron-phonon and electron-electron scattering will modify the wire resistance. Electron-electron scattering in quantum wires is strongly suppressed compared to two- and three-dimensional electron systems. Particularly, in a strictly one-dimensional ideal wire with a single occupied subband it is completely forbidden by energy and momentum conservation.<sup>29</sup> In the presence of inter-subband scattering electron-electron relaxation becomes possible but vanishes in the zero temperature limit together with the scattering by thermal phonons. Elastic scattering will also reduce momentum restrictions and make electron-electron scattering possible. In the following, we suppose that the phase breaking processes will be determined mainly by nonequilibrium phonons, that is by the processes described in Sec. II. If elastic scattering events are more frequent than those of phonon scattering, the electron motion has a diffusive character. For semiquantitative estimates we will assume that all subbands are characterized by the same elastic mean free path  $l$ , diffusion coefficient  $D$ , and electron-phonon rate  $W$ . In this case, we may describe phase relaxation in the wire by a single characteristic relaxation length  $L_\phi = \sqrt{D/W}$ . In the Appendix we discuss briefly more general expressions which allow for different elastic and inelastic scattering rates for the different subbands.

Now it becomes evident that for calculating AC, one must find the dependence of a wire resistivity on the phase relaxation length  $L_\phi$ , the only parameter characterizing the influence of nonequilibrium phonons on the electron system. There is no single universal formula for this dependence and the answer will depend on the relations between the characteristic lengths of the system:  $L$ ,  $L_\phi$ ,  $l$ , and  $l_{loc}$ . It is convenient to classify all possible cases depending on the wire length  $L$ .

### A. Long wires ( $l_{\text{loc}}, L_\phi < L$ )

In wires with  $l_{\text{loc}} < L_\phi < L$ , all electron states are localized<sup>30</sup> and the equilibrium conductivity  $\sigma_0$  at zero temperature must vanish. At nonzero temperatures phonons cause hopping transitions between localized states which results in nonzero  $\sigma_0$ . It is natural to expect that the same transitions can be caused by nonequilibrium phonons as well. As a result, we may expect a positive AC for this case.

In this and the next section we shall use the approach applied in Ref. 33 for calculating the temperature dependence of the wire conductance caused by destruction of localization. To illustrate this, let us suppose that inelastic scattering takes place at a single point  $y_0$ . In this case, electron motion in the regions  $0 < y < y_0$  and  $y_0 < y < L$  becomes uncorrelated and the wire can be considered as two independent wires with lengths  $y_0$  and  $L - y_0$  connected in series. The resistance of each wire is given by the formula Eq. (17). Since the  $r$  vs wire length dependence [Eq. (17)] is superlinear, the conductance of such a composed wire will exceed the value obtained from Eq. (17) for a single wire with length  $L$ . Hence, inelastic scattering increases the wire conductance.

We consider a Poisson time distribution of inelastic scattering events with a mean value  $W^{-1}$ . This means that in our case of a very long wire the inelastic mean free paths (the lengths of independent wires)  $\xi$  are described by the distribution function  $P(\xi) = (2\xi/L_\phi) \exp(-\xi^2/L_\phi^2)$ . The resulting wire resistivity per unit length is determined as a series resistance of these elementary parts and given by the formula

$$\begin{aligned} \rho &= r_s \frac{\int d\xi \xi \exp(-\xi^2/L_\phi^2) [\exp(\xi/l_{\text{loc}}) - 1]}{\int d\xi \xi^2 \exp(-\xi^2/L_\phi^2)} \\ &= \frac{r_s}{l_{\text{loc}}} \exp\left(\frac{L_\phi^2}{4l_{\text{loc}}^2}\right) \left[1 + \Phi\left(\frac{L_\phi}{2l_{\text{loc}}}\right)\right]. \end{aligned} \quad (18)$$

Here  $\Phi(x)$  is the probability integral. The positive sign of  $d\rho/dL_\phi$  results in positive AC. For  $L_\phi \ll l_{\text{loc}}$ , Eq. (18) reduces to the well-known expression for the weak localization correction to the wire conductivity:  $\Delta\sigma \sim -r_s^{-1}L_\phi$  (see, e.g., Ref. 31).

Note that  $L_\phi$  decreases with the sample temperature and, hence, Eq. (18) explains not only positive AC, but also the increase of equilibrium wire conductivity  $\sigma_0$  with the temperature also observed in Ref. 4. Similar temperature behavior in metallic wires was observed in Ref. 32 and treated as a manifestation of localization effects in Ref. 33.

### B. Intermediate wires ( $l < L < l_{\text{loc}}, L_\phi$ )

In this case, the localization term  $\Delta\sigma$  responsible for the positive AC will be a small additional correction to the equilibrium conductance  $\sigma_0 = (r(L))^{-1}$  determined by Eq. (17). If, besides,  $L$  is much less than  $l_{\text{loc}}$ ,  $\sigma_0$  is given by the classical formula:  $\sigma_0 \sim l_{\text{loc}}/(r_s L)$ .

To obtain the expression for  $\Delta\sigma$  in relatively short wires, we shall follow the approach of Ref. 33 for the correction to the conductivity caused by weak localization in wires with  $l < L < l_{\text{loc}}, L_\phi$ . In this case rare inelastic scatterings divide the wire into not more than two independent parts (see Sec. V A). The corresponding corrections to the wire conductance

were calculated by averaging  $y_0$  over the Poisson distribution of inelastic collisions which gave

$$\begin{aligned} \rho &= \frac{r_s}{L} \left[ \exp\left(\frac{L}{l_{\text{loc}}}\right) - 1 \right] \exp\left(-\frac{L^2}{L_\phi^2}\right) + 4 \frac{4r_s}{L_\phi^2} \exp\left(-\frac{L^2}{2L_\phi^2}\right) \\ &\quad \times \int_0^{L/2} dx \left[ \exp\left(\frac{L}{2l_{\text{loc}}}\right) \cosh\left(\frac{x}{l_{\text{loc}}}\right) - 1 \right] \exp\left(-\frac{2x^2}{L_\phi^2}\right). \end{aligned} \quad (19)$$

In the limit  $L \ll l_{\text{loc}}, L_\phi$ , Eq. (19) results in the following  $L_\phi$ -dependent part of the wire conductivity:

$$\Delta\sigma = \frac{L^2}{6r_s L_\phi^2} \sim \frac{e^2 L^2 W}{\hbar D}. \quad (20)$$

The positive AC described by Eq. (20) decreases with the decrease of  $L$ . On the other hand, additional scattering by nonequilibrium phonons will decrease the mean free path  $l$  and, hence, decrease the classical component of conductance. This correction to  $\sigma$

$$\Delta\sigma \sim -\sigma_0 \frac{lW}{v_F} \sim -\frac{e^2 l_{\text{loc}} l W}{\hbar L v_F} \quad (21)$$

increases in magnitude at small  $L$  and, hence, at some critical  $L = L_c$  the crossover from positive to negative AC will take place. By comparing Eqs. (20) and (21), we obtain

$$L_c \sim (l_{\text{loc}} l^2)^{1/3}. \quad (22)$$

Since the expression Eq. (20) used in our estimates is valid only for  $L \ll l_{\text{loc}}$ , one can see that  $L_c$ , in fact, belongs to the region of intermediate wire lengths considered in this section.

### C. Short wires ( $L < l$ )

This case, which includes also ballistic point contacts, corresponds to the ideal wire considered in Sec. III. Formula Eq. (11) gives an adequate description of AC except for the narrow regions where  $E_F \approx E_N$ . To obtain an expression which is valid everywhere, we must perform similar calculations using the self-consistent density of states taking into account the level broadening and calculated in Sec. IV. This procedure suppresses the divergencies at  $E_F = E_N$ . One can see that for short, ballistic wires AC is always negative contrary to the case of long wires.

## VI. PHONON SCATTERING AND PROPERTIES OF POSITIVE AC

In the previous section we have shown that, except for the case of very short wires, AC is positive and grows monotonically with increasing probability of scattering by nonequilibrium phonons  $W_N(k)$ . That is why the main properties of AC and, particularly, its dependence on  $E_F$  (that is on electron concentration) are determined by corresponding properties of  $W_N(k)$ .

Let us now explore in more detail the  $E_F$  dependence of AC. In Fig. 6, we show AC  $\Delta\sigma$  vs  $E_F$  for long wires (see Sec. V A) in the weak localization regime, i.e.,  $L_\phi < L, l_{\text{loc}}$ . Here  $\Delta\sigma$  is given by the weak localization formula derived for two occupied subbands in Appendix Eq. (A11) with the

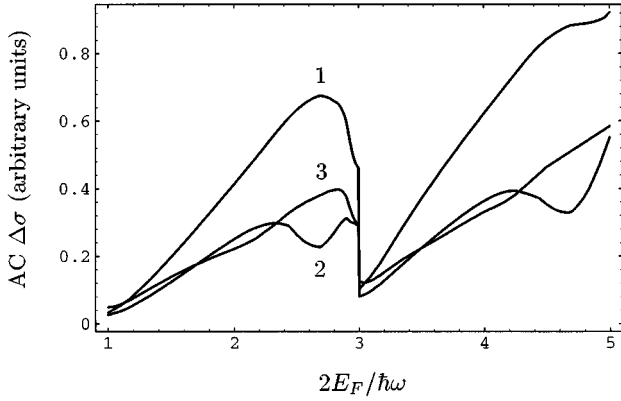


FIG. 6. Fermi energy dependence of AC  $\Delta\sigma$  (arbitrary units) for heater temperature  $T_h = 10^2 m s^{-2}$  and ambient temperature  $T_a = 10 m s^{-2}$ . The wire width parameter  $s\sqrt{m/\hbar\omega}$  is equal to 0.05 (curve 1), 0.1 (curve 2), and 0.3 (curve 3). Note that the sharp transition at  $E_F = 3$  ( $\equiv N=1$  subband edge) would be smoothed somewhat by the inclusion of disorder effects in the phonon rate  $W_N$ .

phase relaxation rate given by  $W_N$  [Eq. (4) and Fig. 1] for the isotropic Bose distribution and the self-consistent relaxation rate  $\tau_N^{-1}$  [Eq. (15) and Fig. 5]. The key features to note, besides the positive sign of AC, are (i) the double peak appearing to the left of a given subband edge for some wire parameters and (ii) the saturation of  $\Delta\sigma$  for a large heater temperature. The latter fact is not seen from Fig. 6 but is confirmed by the calculations of AC at different  $T_h$ .

To understand these features, let us consider the range  $E_F < E_1$  with only one occupied subband. Then  $\Delta\sigma$  is approximately

$$\Delta\sigma \approx -\frac{e^2}{\pi\hbar} v_F \sqrt{\tau_0} (\sqrt{W_{h0}^{-1}} - \sqrt{W_{a0}^{-1}}), \quad (23)$$

where  $W_{h0}$  and  $W_{a0}$  are the  $N=0$  nonequilibrium and ambient electron-phonon rates, respectively. When the heater temperature is much larger than the ambient temperature, we have  $W_{h0}^{-1} \ll W_{a0}^{-1}$  and therefore

$$\Delta\sigma \approx +\frac{e^2}{\pi\hbar} v_F \sqrt{\tau_0} W_{a0}^{-1}, \quad (24)$$

independent of the heater temperature. Equation (24) suggests the possibility of using nonequilibrium phonon pulses to measure directly the absolute value of the weak localization correction.

The double peak in curve 2 is a consequence of the  $E_F$  dependences of *both*  $W_0$  [curve 2 in Fig. 1(b)] and  $\tau_0^{-1}$  (Fig. 5). If  $W_0$  were constant, then from Fig. 5 and Eq. (23) we see that  $\Delta\sigma$  would have a single peak just to the left of  $E_1$ . However, the strong peak in the intersubband rate  $W_{01}$  close to the  $N=1$  subband edge produces a ‘‘dip’’ in the  $\Delta\sigma$  peak, resulting in the double-peak profile. Increasing the wire width smooths the  $W_N$  vs  $E$  dependence [curve 3 in Fig. 1(b)], while decreasing the width suppresses intersubband scattering [curve 1 in Fig. 1(b)] and thus in both limits we expect the dip to vanish, giving just a single peak. Curves

1–3 in the figure show this. Such double-peak features are also apparent in the experimental curve of Ref. 4, lending support to our present model.

It is worth noting that, according to the results of Sec. II B, the character of the AC vs  $E_F$  dependence is sensitive to the angles  $\theta_0, \phi_0$  (see Fig. 4). This means that by shifting the hot spot position (especially along the wire direction), we can change this dependence which is experimentally measured in gated quantum wire structures, such as in Ref. 4.

## VII. CONCLUSION

To summarize, we have shown that the positive AC can be adequately explained by a model of a quantum wire with elastic scatterers causing electron localization which, in turn, is partially suppressed by inelastic phonon scattering. The probability of electron-phonon scattering and, hence, the amplitude of AC oscillates with the Fermi energy  $E_F$  in a wire which can be changed by a gate voltage  $V_G$ . Both a positive sign of AC and its oscillation with  $V_G$  have found their confirmation in the experiment.

In very short wires, as well as in quantum point contacts, the localization effects are of minor importance. In this case, the main effect of phonon scattering will be an increase in the backscattering probability, resulting in negative AC.

Note that not only AC but all characteristic lengths  $l$ ,  $l_{loc}$ , and  $L_\phi$  oscillate with  $E_F$ , acquiring their minimum values at approximately  $E_F \approx E_N$ , where the density of states is a maximum (see also Ref. 17). This is why it is possible by changing the electron concentration for a ‘‘short’’ wire to become ‘‘long’’ and vice versa. In this case AC can change its sign periodically, being positive at  $E_F \approx E_N$  and negative—far from these points.

## ACKNOWLEDGMENTS

The authors are grateful to A. J. Kent who initiated their activity and to Yu. M. Galperin, A. Zyuzin for valuable remarks. Very helpful discussions with A. MacKinnon are also gratefully acknowledged. The work was partially supported by the NATO Grant No. CRG 930040.

## APPENDIX

We give here the derivation of the weak localization correction to the conductivity of a long wire, allowing for the possibility of having more than one subband edge below  $E_F$ . The derivation is a straightforward generalization of the usual one for the single subband case (see, e.g., Ref. 34). Suhrke and Wilke<sup>35</sup> also consider the multisubband case, but neglect the dependence of the elastic scattering rate and phase relaxation rate on the subband index  $M$ . As we shall see below, keeping the  $M$  dependence leads to the additional complication of having to invert a matrix of an order equal to the number of subband edges below  $E_F$ .

Assuming the subband separation is much larger than the disorder broadening, i.e.,

$$E_{M+1} - E_M \gg \frac{\hbar}{\tau_M}, \quad (A1)$$

the one electron Green functions are then approximately diagonal in the quantum number  $M$ :  $G_{MN}^{(\pm)} \approx G_M^{(\pm)} \delta_{MN}$ , where

$$G_M^{(\pm)}(k, E) = \left( E - E_M - \frac{\hbar^2 k^2}{2m} \pm i \frac{\hbar}{2\tau_M(E)} \pm i \frac{\hbar}{2\tau_M^\phi(E)} \right)^{-1}, \quad (\text{A2})$$

with  $\tau_M(E)$  given by Eq. (15) and where  $\tau_M^\phi(E)$  is the phase relaxation time approximately equal to  $W_M^{-1}$  given by Eq. (4). In terms of these one electron Green functions, the weak localization correction at zero temperature is approximately

$$\Delta\sigma \approx \frac{e^2 \hbar^3}{\pi m^2 \Omega^{1/3}} \sum_{M, k, q} k(q-k) G_M^{(+)}(k, E_F) G_M^{(-)}(q-k, E_F) C_M(q, E_F) G_M^{(+)}(q-k, E_F) G_M^{(-)}(q-k, E_F). \quad (\text{A3})$$

The function  $C$  denotes the sum over all maximally crossed diagram contributions to the irreducible vertex function and is given by

$$C_M(q, E) = \sum_{I, J} T_{MI} \Pi_I(q, E) M_{IJ}(q, E) T_{JM}, \quad (\text{A4})$$

where

$$T_{MN} = \frac{N_i |V|^2}{(2\pi)^2 \Omega^{1/3}} \int dq_x dq_z |Z(q_z)|^2 |Q_{MN}(q_x)|^2, \quad (\text{A5})$$

$$\Pi_I(q, E) = \sum_k G_I^{(+)}(k, E) G_I^{(-)}(k-q, E), \quad (\text{A6})$$

and where  $M_{IJ}$  is the solution to the following equation:

$$M_{IJ}(q, E) = \delta_{IJ} + \sum_K T_{IK} \Pi_K(q, E) M_{KJ}(q, E). \quad (\text{A7})$$

Carrying out the sum over  $k$  in Eqs. (A3) and (A6), we obtain modulo numerical factors of order one

$$\Delta\sigma \approx - \frac{e^2}{\pi \hbar} \sum_{M, I, J} \tau_{MI}^{-1} \tau_I \left( \pi^{-1} \int dq M_{IJ}(q) \right) \times \tau_{JM}^{-1} \tau_M^3 \tilde{v}_M^2 \Big|_{E=E_F}, \quad (\text{A8})$$

where

$$M_{IJ}^{-1}(q) \approx \delta_{IJ} - \tau_{IJ}^{-1} \tau_J \left[ 1 - \frac{\tau_J}{\tau_J^\phi} \right] + q^2 \tau_{IJ}^{-1} \tau_J^3 \tilde{v}_J^2, \quad (\text{A9})$$

and

$$\tilde{v}_M = \left[ v_M^4 + \left( \frac{\hbar}{m \tau_M} \right)^2 \right]^{1/4}, \quad (\text{A10})$$

with  $v_M = \sqrt{2(E_F - E_M)/m}$  the ideal wire electron velocity. The term  $\tau_{MN}^{-1}$  denotes the individual scattering rate into the  $N$ th subband [see Eq. (16)]. The final steps are the inversion of Eq. (A9) to obtain  $M_{IJ}$  and the  $q$  integration in Eq. (A8).

Let  $M_{\max}$  denote the highest occupied subband. Then it is possible to show that restricting the ranges of  $M$ ,  $I$ , and  $J$  in Eqs. (A8) and (A9) to  $0, 1, \dots, M_{\max}$  introduces only a small error. For example, when  $M_{\max} = 1$ , we obtain from Eqs. (A8) and (A9)

$$\Delta\sigma \approx - \frac{e^2}{\pi \hbar} \left[ \frac{\tau_{10}^{-1} \tau_0 \tilde{v}_0^2 + \tau_{01}^{-1} \tau_1 \tilde{v}_1^2}{\tau_{10}^{-1} \tau_0^{\phi-1} + \tau_{01}^{-1} \tau_1^{\phi-1}} \right]^{1/2} \Big|_{E=E_F}. \quad (\text{A11})$$

<sup>1</sup>L. J. Challis, A. J. Kent, and V. W. Rampton, *Semicond. Sci. Technol.* **5**, 1179 (1990).  
<sup>2</sup>A. J. Kent, *Physica B* **169**, 356 (1991).  
<sup>3</sup>D. J. McKitterick, A. Shik, A. J. Kent, and M. Henini, *Phys. Rev. B* **49**, 2585 (1994).  
<sup>4</sup>A. J. Naylor, K. R. Strickland, A. J. Kent, and M. Henini, *Surf. Sci.* **362**, 660 (1996).  
<sup>5</sup>S. Briggs and J. P. Leburton, *Phys. Rev. B* **38**, 8163 (1988).  
<sup>6</sup>G. Fishman, *Phys. Rev. B* **36**, 7448 (1987).  
<sup>7</sup>N. Telang and S. Bandyopadhyay, *Appl. Phys. Lett.* **62**, 3161 (1993).  
<sup>8</sup>R. Mickevicius and V. Mitin, *Phys. Rev. B* **48**, 17 194 (1993).  
<sup>9</sup>S. G. Yu, K. W. Kim, M. A. Stroscio, G. J. Iafrate, and A. Bal-lato, *Phys. Rev. B* **50**, 1733 (1994).  
<sup>10</sup>U. Bockelmann and G. Bastard, *Phys. Rev. B* **42**, 8947 (1990).  
<sup>11</sup>A. Y. Shik and L. J. Challis, *Phys. Rev. B* **47**, 2082 (1993).  
<sup>12</sup>V. F. Gantmakher and Y. B. Levinson, *Carrier Scattering in Met-als and Semiconductors* (North-Holland, New York, 1987).  
<sup>13</sup>M. Buttiker, in *Electronic Properties of Multilayers and Low-Dimensional Semiconductor Structures*, edited by J. M. Cham-berlain, L. Eaves, and J.-C. Portal (Plenum Press, New York, 1990), p. 51.

<sup>14</sup>V. L. Gurevich, V. B. Pevzner, and K. Hess, *J. Phys. Condens. Matter* **6**, 8363 (1994).  
<sup>15</sup>V. L. Gurevich, V. B. Pevzner, and K. Hess, *Phys. Rev. B* **51**, 5219 (1995).  
<sup>16</sup>H. Bruus, K. Flensberg, and H. Smith, *Phys. Rev. B* **48**, 11 144 (1993).  
<sup>17</sup>D. Liu and S. Das Sarma, *Phys. Rev. B* **51**, 13 821 (1995).  
<sup>18</sup>C. S. Chu and R. S. Sorbello, *Phys. Rev. B* **40**, 5941 (1989).  
<sup>19</sup>J. Masek, P. Lipavsky, and B. Kramer, *J. Phys. Condens. Matter* **1**, 6395 (1989).  
<sup>20</sup>P. Bagwell, *Phys. Rev. B* **41**, 10 354 (1990).  
<sup>21</sup>I. Kander, Y. Imry, and U. Sivan, *Phys. Rev. B* **41**, 12 941 (1990).  
<sup>22</sup>E. Tekman and S. Ciraci, *Phys. Rev. B* **42**, 9098 (1990).  
<sup>23</sup>L. H. Wang, S. C. Feng, F. N. Zeng, and Y. Zhu, *Phys. Lett. A* **165**, 451 (1992).  
<sup>24</sup>T. Ando, A. B. Fowler, and F. Stern, *Rev. Mod. Phys.* **54**, 437 (1982).  
<sup>25</sup>M. J. Kearney and P. N. Butcher, *J. Phys. C* **20**, 47 (1987).  
<sup>26</sup>S. Das Sarma and X. C. Xie, *Phys. Rev. B* **35**, 9875 (1987).  
<sup>27</sup>A. Schmid, *Z. Phys.* **259**, 421 (1973).

- <sup>28</sup>P. W. Anderson, *Phys. Rev. B* **23**, 4828 (1981).
- <sup>29</sup>J. P. Leburton, S. Briggs, and D. Jovanovic, *Superlatt. Microstruct.* **8**, 209 (1990).
- <sup>30</sup>N. F. Mott and W. D. Twose, *Adv. Phys.* **10**, 107 (1961).
- <sup>31</sup>B. L. Al'tshuler and A. G. Aronov, *Pis'ma Zh. Éksp. Teor. Fiz.* **33**, 515 (1981) [*JETP Lett.* **33**, 499 (1981)].
- <sup>32</sup>Z.-Z. Yu, M. Haerle, J. W. Zwart, J. Bass, W. P. Pratt, and P. A. Schroeder, *Phys. Rev. Lett.* **52**, 368 (1984).
- <sup>33</sup>M. E. Farrell, M. F. Bishop, N. Kumar, and W. E. Lawrence, *Phys. Rev. B* **42**, 3260 (1990).
- <sup>34</sup>G. Bergmann, *Phys. Rep.* **107**, 1 (1984).
- <sup>35</sup>M. Suhrke and S. Wilke, *Phys. Rev. B* **46**, 2400 (1992).